



Isostasy, dynamic topography, and the elevation of the Apennines of Italy



Claudio Faccenna^{a,*}, Thorsten W. Becker^b, Meghan S. Miller^b, Enrico Serpelloni^c, Sean D. Willett^d

^a Laboratory Experimental Tectonics, Università Roma TRE, Roma, Italy

^b Department of Earth Sciences, University of Southern California, Los Angeles, CA, USA

^c Istituto Nazionale Geofisica e Vulcanologia, Centro Nazionale Terremoti, Bologna, Italy

^d Department of Earth Sciences, Swiss Federal Institute of Technology, Zurich, Switzerland

ARTICLE INFO

Article history:

Received 19 March 2014

Received in revised form 28 August 2014

Accepted 14 September 2014

Available online xxxx

Editor: Y. Ricard

Keywords:

Apennines

elevation

subduction

isostasy

ABSTRACT

The elevation of an orogenic belt is commonly related to crustal/lithosphere thickening. Here, we discuss the Apennines as an example to show that topography at a plate margin may be controlled not only by isostatic adjustment but also by dynamic, mantle-driven processes. Using recent structural constraints for the crust and mantle we find that the expected crustal isostatic component explains only a fraction of the topography of the belt, indicating positive residual topography in the central Apennines and negative residual topography in the northern Apennines and Calabria. The trend of the residual topography matches the mantle flow induced dynamic topography estimated from regional tomography models. We infer that a large fraction of the Apennines topography is related to mantle dynamics, producing relative upwellings in the central Apennines and downwellings in the northern Apennines and Calabria where subduction is still ongoing. Comparison between geodetic and geological data on vertical motions indicates that this dynamic process started in the early Pleistocene and the resulting uplift appears related to the formation and enlargement of a slab window below the central Apennines. The case of the Apennines shows that at convergent margins the elevation of a mountain belt may be significantly different from that predicted solely by crustal isostasy and that a large fraction of the elevation and its rate of change are dynamically controlled by mantle convection.

© 2014 Elsevier B.V. All rights reserved.

1. Introduction

The Apennine Mountains of Italy comprise an active orogenic belt, with a high-relief, but moderate topographic expression that has formed as a consequence of subduction of the Adriatic plate (Fig. 1; Malinverno and Ryan, 1986; Patacca et al., 1990; Royden, 1993). Although the tectonic setting is well understood, the actual mechanisms of the formation of topography are complex and still debated. Subduction leads to crustal thickening and isostatic uplift (Bally et al., 1986; Casero et al., 1991; Mele et al., 2006) but also produces a complex mantle dynamic response including upwelling (D'Agostino and McKenzie, 1999; D'Agostino et al., 2001), lateral flow (Carminati and Doglioni, 2012), or small-scale convection (Shaw and Pysklywec, 2007; Faccenna and Becker, 2010). It has also been argued that the Adriatic slab is no longer intact

as the slab has detached in the central and southern Apennines leading to regionally enhanced uplift (Wortel and Spakman, 2000; Gvirtzman and Nur, 2001; Faure Walker et al., 2012).

Subduction also induces an isostatic effect due to the subducting lithosphere. This effect is not accounted for by simple local isostasy of the crust. Stresses associated with the negative buoyancy of the dense slab are transmitted up the slab and into both the forearc of the overlying plate and the foreland on the subducting plate (Mitrovica et al., 1989; Karner and Watts, 1983; Royden, 1993). This leads to an isostatic depression of the overlying regions and changes in the slab load or geometry can lead to uplift or subsidence of the overlying regions. Subduction also induces mantle flow and thereby dynamic topography, here defined as the topography due to the radial tractions as exerted by currently active asthenospheric flow. Hence, the topographic and uplift signal of subduction depends on processes including slab sinking (Mitrovica et al., 1989), slab rollback (Carminati et al., 2003; Carminati and Doglioni, 2012), slab break off (Wortel and

* Corresponding author.

Spakman, 2000), and slab-induced return flow (Faccenna and Becker, 2010).

Constraints on the geodynamics of the Apennines come from observations of both topography and surface uplift rates. Topography data are readily available and can be directly compared to crustal and lithospheric density structure in order to differentiate between isostatic and dynamic sources (Royden, 1993; Gvirtzman and Nur, 2001; Carminati and Doglioni, 2012). Uplift rates are constrained by vertical geodetic displacements measured on decadal timescales (D'Anastasio et al., 2006; Devoti et al., 2011; Cenni et al., 2013) and by geomorphic data such as marine terraces on timescales of the order of 10^5 to 10^6 yrs (Ferranti et al., 2006). Recently, Serpelloni et al. (2013) presented a new dense geodetic, vertical velocity solution based on > 800 permanent GPS stations from across the Mediterranean; this effort presents an opportunity for renewed study of uplift rates across several temporal and spatial scales in the Apennines.

In this paper, we consider contributions to topography and uplift rates from both static, lithospheric and dynamic, deeper mantle sources. To constrain the isostatic component of the topography, we use the structure of the crust and lithosphere as inferred from recent receiver function measurements (Mele et al., 2006; Piana Agostinetti and Amato, 2009; Müller and Piana Agostinetti, 2012). To estimate the dynamic topography from mantle flow, we calculate flow velocities from density anomalies based on different seismic tomography models. Topography estimates are then compared with geodetic and geological data to infer uplift and subsidence histories. The result of this comparative analysis is used to quantify the relative contribution of isostatic and dynamic components, providing new insights on the range of subduction processes contributing to the topography and vertical motion of the Apennines mountain belt.

2. Isostasy, elevation and uplift rate

The elevation of a mountain belt and rate of surface uplift are inherently linked, one being the time derivative of the other, and as such they represent the components of mountain belt dynamics that are sensitive to lithospheric structure and rates of change, respectively. Elevation is often argued to be dominated by isostasy of the crust, which, in convergent mountain belts is typically thickened in response to crustal shortening. The lithospheric mantle may also thicken or thin by tectonic processes, and may be subject to localized removal given that its density is slightly higher than that of the underlying asthenosphere (e.g. Houseman et al., 1981; Gvirtzman and Nur, 2001). A thicker lithospheric mantle layer implies lower elevation of the overlying surface. In addition to the static component of topography, another component of elevation may arise due to density anomalies and resultant flow of the deeper mantle, what is commonly referred to as dynamic topography. Vertical flow in the mantle induces stress on the base of the lithosphere and dynamic topography is the result of surface uplift to balance that stress.

Ignoring elastic flexure, which is valid for loads at length-scales larger than the flexural wavelength, the local elevation in a mountain belt (Z) can be described as a combination of an isostatic (z_{iso}) and a dynamic component (z_{dyn}). The isostatic elevation (z_{iso}) depends only on the density structure of the lithosphere and that of the underlying fluid asthenosphere. The elevation of a lithospheric column with respect to a reference elevation (H), usually taken as the average mid-oceanic ridge elevation or any reference datum (2.4 km in Lachenbuch and Morgan, 1990), is given by the lithosphere buoyancy, with components from the crustal layer with a thickness (l_c) and density (ρ_c) and the mantle lithosphere with a thickness (l_m) and density (ρ_m), floating over an asthenosphere of density (ρ_a).

$$z_{iso} = (f_1 l_c + f_2 l_m) - H \quad (1)$$

where $f_1 = (\rho_a - \rho_c)/\rho_a$ and $f_2 = (\rho_a - \rho_m)/\rho_a$. The dynamic topography component (z_{dyn}) may be inferred from stress generated at the base of the lithosphere which is generally estimated by calculating the instantaneous mantle flow due to density anomalies in the mantle as inferred from seismic tomography models (e.g. Ricard et al., 1984; Panasyuk and Hager, 2000).

Surface uplift rate, defined as the time derivative of the Earth's surface (we use the term uplift rate to denote a vertical velocity, positive or negative), similarly, has sources from the deep mantle, lithosphere, and crust. Temporal changes in mantle flow result in changes of dynamic topography and surface uplift. Temporal changes in crustal or lithospheric thickness, and the isostatic adjustment to these, likewise lead to changes in elevation and surface uplift. One of the fastest mechanisms for changing crustal thickness is surface erosion and its negative counterpart, sediment deposition. Isostatic response to erosion or deposition is often a large component of surface uplift rate (Molnar and England, 1990).

As above, the vertical velocity or uplift rate of the surface (V_{surf}) can be decomposed into isostatic (V_{Siso}) and dynamic components (V_{dyn}). The velocity resulting from the isostatic component can be broken down further in terms of the structural thickening rate of crust and lithospheric mantle and the rate of erosion (\dot{e}) and rate of sedimentation (\dot{d}), both of which are taken to be positive, and which cannot coexist at the same point. The isostatic uplift rate of the surface is given by:

$$V_{Siso} = f_1 \frac{dl_c}{dt} + f_2 \frac{dl_m}{dt} - f_1 \dot{e} + f_3 \dot{d}, \quad (2)$$

where we introduce the isostatic factor accounting for the density of sediment as $f_3 = (\rho_a - \rho_s)/\rho_a$.

Eq. (2) is the velocity for the surface of the earth, not the rock at the surface of the earth. In the presence of erosion or deposition, the rock moves at a velocity different from that of the surface, and is defined by:

$$V_{Riso} = f_1 \frac{dl_c}{dt} + f_2 \frac{dl_m}{dt} - (1 + f_1)\dot{e} + (f_3 - 1)\dot{d}. \quad (3)$$

This is the quantity that is measured at geodetic monuments and by geomorphic markers such as marine terraces.

The dynamic component to uplift rate can be defined as the rate of change of dynamic topography and contributes equally to both surface and rock uplift, so that the vertical velocity of the surface and of the rock at the surface are obtained by adding this to Eq. (2) or (3), respectively, giving expressions for surface and rock uplift as:

$$V_S = f_1 \frac{dl_c}{dt} + f_2 \frac{dl_m}{dt} - f_1 \dot{e} + f_3 \dot{d} + \frac{dz_{dyn}}{dt} \quad (4)$$

and

$$V_R = f_1 \frac{dl_c}{dt} + f_2 \frac{dl_m}{dt} - (1 + f_1)\dot{e} + (f_3 - 1)\dot{d} + \frac{dz_{dyn}}{dt}. \quad (5)$$

Observations of topography and rock uplift rate must therefore differentiate between the processes implicit to each of the terms in these expressions. To determine the isostatic and dynamic components, we must estimate the density structure of the lithosphere and the motion of the mantle. To resolve the components of the uplift rate, we must estimate erosion and sedimentation rates, crustal thickening or thinning rates and components of dynamic topography, including glacial isostatic adjustment from ice sheet melting and water loading.

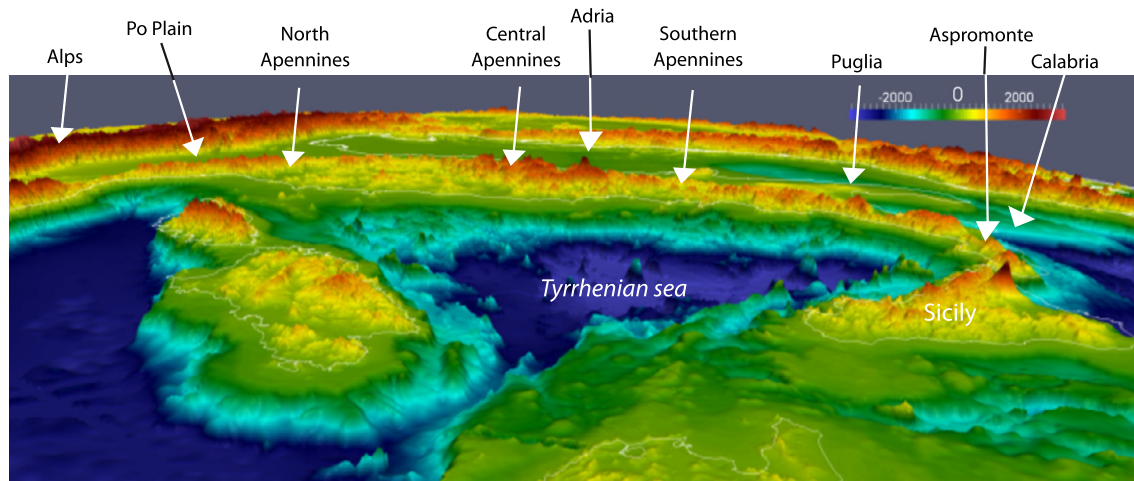


Fig. 1. Oblique view of the Apennines system topography with strong vertical exaggeration. Note the elevation of the Central Apennines and other geographic features.

3. Geological background of the Apennines belt

The Italian peninsula extends for more than ~ 1000 km within the central Mediterranean, forming a narrow (< 200 km) mountain belt, the Apennines–Calabria, from the Alps to Sicily (Fig. 1). The belt itself is formed by slices of upper crustal material, scraped off from the downgoing Adriatic and Ionian plates, and stacked beneath the upper Tyrrhenian plate during the Neogene (Malinverno and Ryan, 1986; Patacca et al., 1990). As a result, beneath the Apennines crest, the crust is up to ~ 40 – 50 km thick, ~ 1.5 thicker than the undeformed Adriatic crust (Piana Agostinetti and Amato, 2009; Figs. 2e and 3). The Apennines thus define a crustal orogenic wedge grown by crustal thickening during the Neogene (Casero et al., 1991; Bally et al., 1986; Mostardini and Merlini, 1986). On its retro-wedge side (west) the Apennines wedge is under extension, with east and west dipping normal faults, creating marine and intramontane basins (e.g. Cavinato and De Celles, 1999; D’Agostino et al., 2001, 2011a, 2011b; Bennett et al., 2012; Angelica et al., 2013) (Figs. 2c, 3). Extension produces a thinning of the upper Tyrrhenian plate that has led to the break-up and the emplacement of oceanic crust in the southern Tyrrhenian (Patacca et al., 1990; Kastens et al., 1988). Compression is limited to the pro-wedge external region, off the Adriatic–Ionian coast and the frontal regions of the Northern Apennines on the border of the Po Plain, with evidence from geological structures and seismicity (Doglioni et al., 1999; Minelli and Faccenna, 2010; Chiarabba et al., 2005; Bennett et al., 2012). Conversely, there is no clear evidence of compression along the front of the Central Apennines; here, convergence has been inferred to have ceased in the Lower–Middle Pleistocene (Patacca et al., 1990; Montone et al., 2004). Compression in the Calabrian arc is observed only in the most recently deformed part of the Ionian wedge (Gutscher et al., 2006; Minelli and Faccenna, 2010), and evidence from geodesy is more elusive (Serpelloni et al., 2010).

The style of crustal accretion varies between the Apennines and Calabria, as sediments available for accretion decrease to the south, where the deep Ionian basin is floored by oceanic lithosphere (e.g. Minelli and Faccenna, 2010, and references therein). The elevation of the mountain belt reflects the tectonics. The Apennines and Calabria exhibit a low-taper pro-wedge increasing in elevation westward to the crest, west of which normal faults are active. The retro-wedge side has been lowered by this extension (Figs. 2 and 3), tapering to the Tyrrhenian Sea. The mean elevation of the Italian peninsula is ~ 400 – 500 m, with higher mean elevation value in the Central Apennines (~ 600 m) and lower in the Northern Apennines (~ 300 m) and Calabria (~ 100 m) (Figs. 2a and 3b).

4. Topography and vertical motion of the Apennines: geodetic and geological constraints

To estimate the present-day Apennines–Calabria vertical motion, we considered a three-dimensional geodetic solution obtained from the analysis of position time-series of > 800 continuous GPS stations in the European–Mediterranean area (Serpelloni et al., 2013); more than 350 of these sites are located on the Italian peninsula between the Po Plain and Sicily (Figs. 2b, 3a), and are given in the Supplementary material. We refer to Serpelloni et al. (2013) for the details of the processing and post-processing procedures adopted to estimate velocities and uncertainties. The velocities have been obtained from the analysis of the time series of 2.5 to 14 yrs of positions, where the spatially correlated common mode error has been removed. The time series are realized in the IGS08 reference frame, which is the GPS-based realization of the global secular frame ITRF08, so that vertical motions are with respect to the Earth-system center of mass to ± 0.5 mm/yr (Altamimi et al., 2011).

The vertical motions due to glacial isostatic adjustment (GIA) at GPS sites have been estimated considering two global GIA models (Peltier, 2004; Lambeck et al., 1988) (Fig. 2). Both models predict a long wavelength pattern of subsidence in the central Mediterranean. Thus, correction of the GPS velocities for the GIA contribution implies increased rates of tectonic uplift (Fig. S1). The two global models provide GIA estimates that differ by up to 0.5 mm/yr in southern Italy, and this difference can be considered as a rough estimate of uncertainties associated with GIA modelling in the Mediterranean.

Overall, the geodetically inferred vertical motions resemble the long wavelength (> 150 km) topography (Figs. 3a, 3b): the maximum uplift rate across strike occurs near the Apennine divide, and subsidence, or slower uplift rate, is observed in the Tyrrhenian and Adriatic domains (Fig. 2b). Along strike, uplift is observed in the central–southern Apennines decreasing both northward, towards the northern Apennines and Po Plain, and southward, towards Calabria and the southern Tyrrhenian (Fig. 4). The Po Plain and the northern Tyrrhenian are subsiding, but the northern Apennines are uplifting slowly (Fig. 2b). In southern Italy, Calabria shows overall subsidence (Fig. 3a), with rapid subsidence on the western (Tyrrhenian) side and slow uplift of the eastern (Ionian) side. Similarly, southern Sicily shows slow subsidence rates with a transition to modest uplift rates in northern Sicily.

In the northern and central Apennines, the GPS observations may be compared with estimates obtained from levelling data (D’Anastasio et al., 2006), which span a much longer time-interval

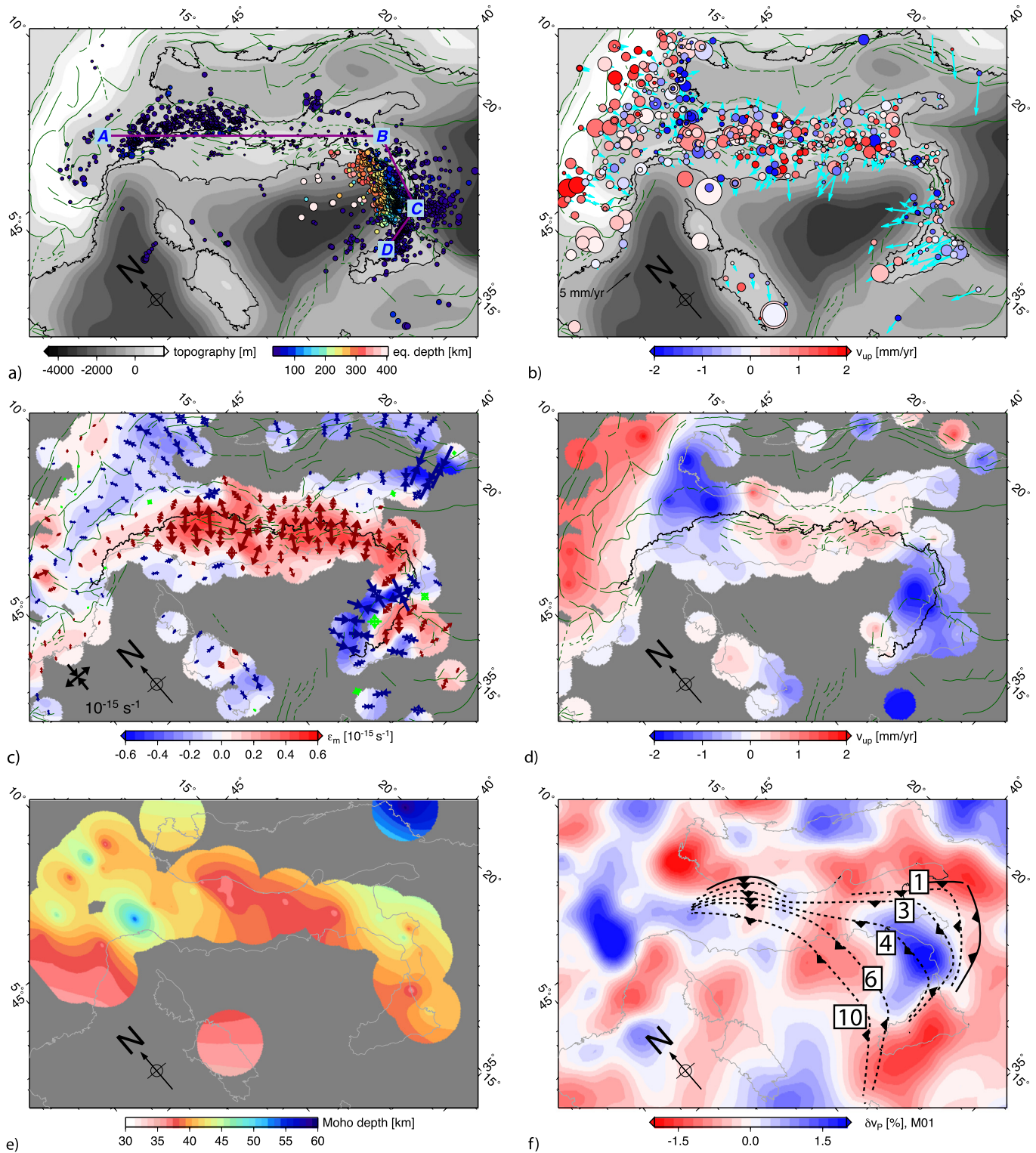


Fig. 2. Structural, morphological and kinematic features of the Apennines–Calabria belt. a) Topography (gray scale), seismicity (deeper than 30 km; color-coded by depth) from the Italian Permanent Seismic Network catalogue (Chiarabba et al., 2005), along with the profile locations used in Fig. 2 in magenta. Black lines represent the topographic divide between the Tyrrhenian and the Adriatic drainage basins. b) Vertical velocity estimates from GPS, circle radii scale with the inverse of the error bar on the vertical, background is smoothed topography (Gaussian filter convolved, wavelength $> \sim 150$ km) as used for the swath in the profile plots in Fig. 2, along with horizontals from GPS (light blue vectors), in an Apennines fixed reference frame, defined by minimizing the horizontal velocities inside a ± 50 km swath profile (A–B). c) Horizontal strain-rate from same geodetic data as from 2b, blue is compressional and red is extensional mean normal strain-rate. d) Vertical velocity as smoothed from the original geodetic data and used in profiles, and trace of the main active normal faults. e) Colored contoured Moho depths greater than 35 km from the merged S and P receiver function based estimates (Piana Agostinetti and Amato, 2009; Miller and Piana Agostinetti, 2012). f) Average (50–300 km depth) uppermost mantle tomography from the M01 P wave tomography model (Piromallo and Morelli, 2003). Dashed black line indicates the position of the trench (where number is time in Myrs) and solid black line indicates the present day trench (Faccenna et al., 2005).

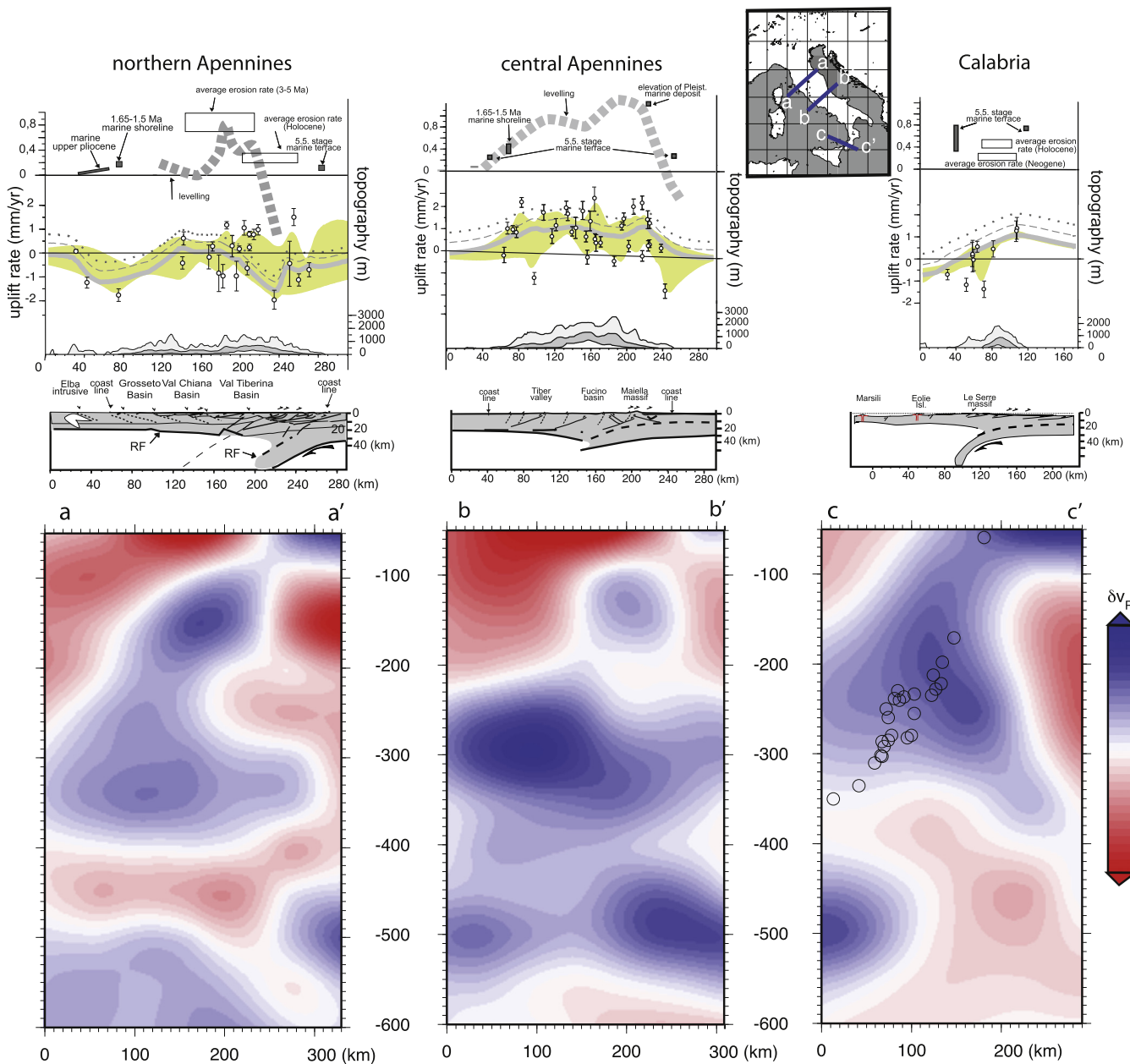


Fig. 3. Representative cross section along the (a) Northern, (b) Central Apennines and (c) Calabria (location in the inset). For each profile we show the swath and the GPS data (average value in grey line), and GIA correction models (ICE-5G, [Peltier, 2004](#): dark green continuous line; KL05, [Lambeck et al., 1988](#): dark green dashed line; modified from [Serpelloni et al., 2013](#)) (100 km wide strip), the levelling data (dashed thick grey line, [D'Anastasio et al., 2006](#)) geological data (upper panel). Erosion data are from: [Bartolini et al. \(1996\)](#); [Cyr and Granger \(2008\)](#); [Thomson \(1998\)](#); [Thomson et al. \(2010\)](#) and [Olivetti et al. \(2012\)](#); uplift rate from marine deposits from: [Ferranti et al. \(2006\)](#); [Pizzi \(2003\)](#); [D'Anastasio et al. \(2006\)](#). Cross sections: a) modified from [Pauselli et al. \(2006\)](#) and [Piana Agostinetti et al. \(2011\)](#) for the deep structure; b) [Di Luzio et al. \(2009\)](#) and [Miller and Piana Agostinetti \(2012\)](#) for the deep structure; c) modified from [Faccenna et al. \(2011\)](#) and [Piana Agostinetti et al. \(2009\)](#) for the deep structure.

(1950–1990) than the GPS data (1998–2011). Vertical velocities from levelling in [D'Anastasio et al. \(2006\)](#) refer to the tide gauge of Genova, where the GPS velocity (at the site GENO) is -0.18 ± 0.15 mm/yr; so there should not be large systematic differences between the two vertical velocity fields. However, the rates from levelling data in [D'Anastasio et al. \(2006\)](#) are no longer available, so here we compare only the general patterns of the geodetic profiles across the Apennines ([Fig. 3](#)). On the central Apennines section, the pattern of the two sets of data show a reasonable agreement, exhibiting an asymmetric dome-shape with an average uplift rate of ~ 1 mm/yr. On the northern Apennines section, uplift rates are slower than in the central Apennines with subsidence on the Tyrrhenian side and in the Po Plain, consistent with the GPS data. The Adriatic slope of the Apennines is

more complicated with subsidence of the mountain front evident in both the GPS and levelling data close to Adriatic coast of our profile ([Fig. 3](#)), but regions both north and south of Rimini show slow uplift of the mountains with a hinge at the mountain front, separating the uplifting mountains from the subsiding Po Plain.

Geological markers providing longer term vertical motion rates within the Apennines are present, but are limited to the external edges of the belt. The presence along the Apennines of marine Pliocene deposits standing at different elevations and attitude indicate that the chain has uplifted during the Pleistocene ([Bartolini et al., 2003](#)). Stage 5.5 (~ 125 kyr) marine terraces on the eastern Adriatic–Ionian shoreline are elevated, with an uplift rate peak in Calabria of ~ 0.8 mm/yr and decreasing toward Puglia

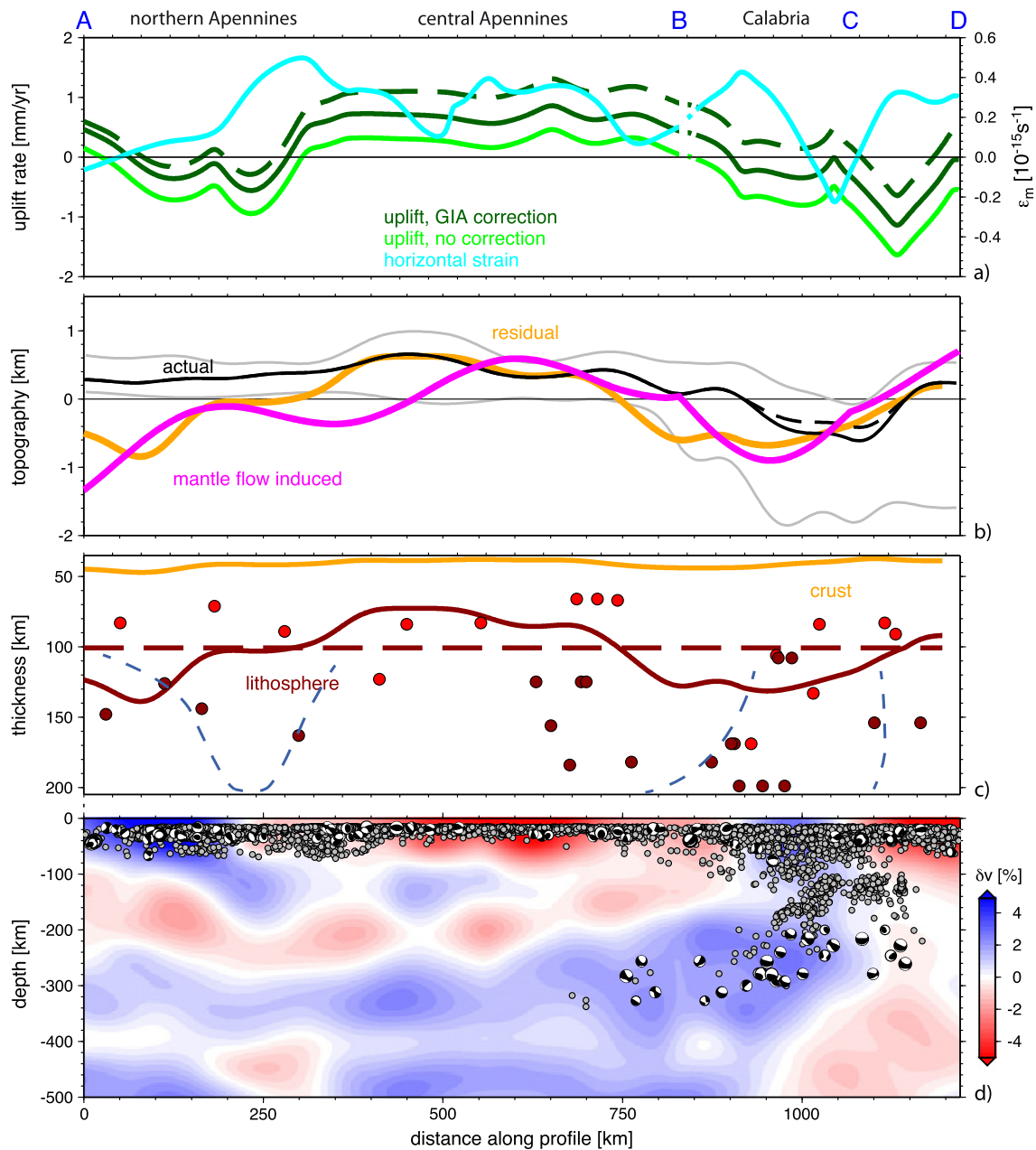


Fig. 4. Topography, geodetic velocity, and structure along the strike of the Apennines–Calabria belt, following the profiles in Fig. 2a. a) Smoothed vertical geodetic velocities (light green) and relative glacial isostatic (GIA) correction models: (ICE-5G (Peltier, 2004): dark green continuous line; KL05 (Lambeck et al., 1988): dark green dashed line). Light blue line shows the mean horizontal strain rate from smooth interpolation of geodesy as in Fig. 2c. b) Median (black), minimum and maximum (grey) topography from a ± 75 km swath along profile for the >150 km filtered topography shown in Fig. 2b; residual topography subtracting a 100 km thick lithospheric column from actual topography (orange), and mantle flow induced topography estimates from the M01 tomographic model (Piromallo and Morelli, 2003). c) Crustal thickness (orange line) from P and S wave receiver function based estimates (Piana Agostinetti and Amato, 2009; Miller and Piana Agostinetti, 2012) greater than >35 km to ignore the Tyrrhenian Moho (Fig. 2c); lithosphere thickness used to estimate residual topography (brown dashed line); lithosphere thickness needed to obtain zero residual topography (brown continuous line) along with T2 (red dots) and T3 (brown dots) negative phases from SRFs (Miller and Piana Agostinetti, 2012) indicating the LAB of the overriding and subducted lithosphere, respectively, projected onto the profile; blue dashed line depicts the boundaries of the high velocity anomalies for the Calabrian and Northern Apennines slabs, as in d). d) Seismicity (Chiarabba et al., 2005), focal mechanisms (gCMT catalog), and M01 tomographic model (Piromallo and Morelli, 2003).

(~ 0.15 mm/yr), and to a lesser degree in the northern Adriatic (~ 0.07 mm/yr), up to the northern Adriatic–Po Plain where those deposits are below sea-level, indicating a negative uplift rate of ~ -0.9 mm/yr (Ferranti et al., 2006) (Fig. 3). Obtaining uplift rate data from stage 5.5 deposits on the Tyrrhenian side of the mountain belt is problematic as many are locally affected by normal faulting. Marine lower Pleistocene deposits at ~ 700 m elevation on the eastern flank of the central Apennines constrain uplift rate post 0.7 Ma as ~ 1 mm/yr (Pizzi, 2003), which is in good agree-

ment with geodetic estimates. In the northern Apennines, uplift rates have been estimated to be ~ 0.6 mm/yr since the Middle Pleistocene (Bigi et al., 2003). In summary, both geodetic and geological data from the Apennines belt show significant differences in topography and uplift rates both across and along strike. The central Apennines are higher and uplifting at higher rates than the northern Apennines and Calabria. Regions of subsidence on the range flanks in both the Northern Tyrrhenian and the Po–Adriatic are not present in the central Apennines.

5. Lithosphere and mantle structure and the expected elevation of the Apennines

To understand the origin of the lateral variations of topography and uplift rates along the Apennines, we examine the crustal and mantle structure. The Moho depth beneath the Apennines is well constrained by active source seismic data (see Scrocca et al., 2003 and references therein), receiver functions (Piana Agostinetti and Amato, 2009; Bianchi et al., 2010), and shallow tomography studies (Di Stefano et al., 2011). The results of these studies show that the Adriatic crust is on average ~30–35 km thick and reaches a maximum depth of ~40–50 km subducting beneath the upper plate (Tyrrhenian) where the Moho is at ~20–25 km depth. Beneath the Northern Apennines and Calabria, the maximum crustal thickness is ~50 km, whereas beneath the Central–Southern Apennines it is limited to ~40 km. Fig. 2e shows these variations of the Adriatic Moho along the strike of the Apennines–Calabria–Sicily derived from merging *P* and *S*-RF (Piana Agostinetti and Amato, 2009; Miller and Piana Agostinetti, 2012), excluding the shallow layer estimates that are associated with the Moho of the upper plate.

Upper mantle structure can be inferred from seismicity and seismic tomography. Deep seismicity is found beneath Calabria, where a steeply dipping Wadati–Benioff zone is defined down to ~500 km. Intermediate depth seismicity is found beneath the Northern Apennines, limited to a depth of ~100 km (Chiarabba et al., 2005) (Figs. 2a, 3c). Between these two clusters, no sub-crustal seismicity has been detected. Tomographic models show steeply dipping high velocity perturbations beneath the Northern Apennines and Calabria, where the slab penetrates into the transition zone (Lucente et al., 1999; Wortel and Spakman, 2000; Piromallo and Morelli, 2003). Beneath the Central–Southern Apennines, no high velocity zone is observed, but, rather, anomalous low velocities are detected in a zone extending into the shallow upper mantle to an upper level estimated to be at ~80 km (Giacomuzzi et al., 2012); 150 km (Lucente et al., 1999; Piromallo and Morelli, 2003) or 200 km (Wortel and Spakman, 2000) (Fig. 3b, S3). Fig. 2f shows *P* wave velocity anomalies averaged for uppermost mantle 40–300 km depths (Piromallo and Morelli, 2003). *S* wave *RF* studies also show two discontinuities that may be correlated with the base (“lithosphere–asthenosphere boundary”, LAB) of the Tyrrhenian plate and, at greater depths, of the Adriatic subducted lithosphere (Miller and Piana Agostinetti, 2012).

We use seismology based crustal thickness estimates to determine the expected elevation of the Apennines from a lithospheric isostatic balance. Using the crustal thickness estimates shown in Figs. 2e and 4 (Chiarabba et al., 2005) and a 100 km thick lithosphere (average lithosphere thickness from *S*-RF by Miller and Piana Agostinetti, 2012) to match the observed topography at crustal (ρ_c) and mantle lithosphere (ρ_m) densities of 2850 kg/m³ and 3250 kg/m³, respectively requires an asthenospheric density (ρ_a) of 3180 kg/m³. The resulting residual topography, derived from the difference between the observed and Airy isostatic topography, resembles an emphasized version of the actual topography (Fig. 4b). Residual topography is negative in the northern Apennines and in Calabria, with maximum amplitude of ~−800 m, and positive in the central Apennines, with an amplitude of up to ~600 m. This suggests that the northern Apennines and Calabria should stand higher than the observed elevation and the central Apennines should stand at a relatively lower elevation relative to the profile. Alternatively, we can assume Airy isostatic equilibrium, but calculate the lithospheric mantle thickness required to achieve zero residual topography (Fig. 4c; Miller and Piana Agostinetti, 2012). As expected, the lithospheric root would be thicker (~80–90 km) and at greater depth (~130–140 km) beneath the northern Apennines and Calabria and thinner (~40 km) and shallower (~80 km) beneath the central Apennines. *S*-RF analysis shows the presence of

deep, negative velocity contrasts beneath the northern Apennines and Calabria at ~150 and ~170 km depth, respectively, interpreted as the conversion of *S*-to-*P* at the base of the subducted lithosphere (Miller and Piana Agostinetti, 2012; Fig. 4c). Therefore, one could reasonably consider that a reconstructed ~140 km deep mantle root, placed on seismically active regions in the northern Apennines and Calabria, represents the base of the Adriatic–Ionian subducting lithosphere, actively pulling down the belt, depressing its topography by ~600 m.

To quantitatively test the idea that the subducting slab and its evolution may influence the topography, we estimate the expected dynamic component of topography (Z_{dyn}) induced by instantaneous mantle flow due to density anomalies in the mantle as inferred from *P* wave seismic tomography models (Piromallo and Morelli, 2003). This deflection may be inferred from instantaneous mantle flow from the radial tractions acting upon a free-slip surface boundary in an incompressible, Newtonian fluid spherical annulus that has only radial viscosity variations (for details, see Becker et al., 2014). These approximations allow for a semi-analytical approach to estimate global mantle flow based on spectral methods. The density model was constructed by scaling the seismic velocity structure into temperature (e.g., Hager, 1984; Gurnis et al., 2000; Ricard et al., 1984, 1993; Hager et al., 1985; Le Stunff and Ricard, 1995; Panasyuk and Hager, 2000; Simmons et al., 2010; Steinberger and Calderwood, 2006; Becker and Faccenna, 2011). Results show that dynamic topography is positive in the central Apennines, reaching a peak of ~400 m, almost null in the northern Apennines, and negative in the Po Plain and in Calabria (~−600 m or more negative) (Fig. 4b).

A similar trend is confirmed by adopting other tomography models (Fig. S2). In particular, results from the CG12S v_S model of Giacomuzzi et al. (2012) are comparable to those from M01 shown in Fig. 4. Results based on v_P from MIT08 (Li et al., 2008) and CG12P (Giacomuzzi et al., 2012) show a similar trend with respect to M01 but shifted up (~500 m) or down (~−500 m), respectively (Fig. S3). These tests confirm that the uncertainties, such as those arising from scaling velocity anomalies to density, or due to different imaging resolution of tomography, can be expected to lead to uncertainties with respect to absolute values of inferred dynamic topography. However, the overall trend is robust, and geographic patterns appear associated with the along strike variations of the degree to which subduction is active along the Apennines. Moreover, the good overall correlation between the dynamic topography and the residual component of topography indicates that at least part of the topography may be produced by stresses related to mantle convection.

6. Discussion

6.1. The Apennines topography

The Apennines are a complex mountain range with diverse tectonic and geodynamic processes active, and determining the relative importance of these processes to the building of topography is difficult. Crustal thickening of the orogenic wedge and crust is well established, as is crustal thinning by extension, but it has been argued that the topography and the current uplift rates are also affected by deeper mantle geodynamic processes such as slab break-off or delamination (Westway, 1993; Wortel and Spakman, 2000; Gvirtzman and Nur, 2001), mantle upwelling in Central Apennines (D’Agostino and McKenzie, 1999), toroidal flow around the narrow Calabrian slab (Faccenna et al., 2005, 2011; Faccenna and Becker, 2010), and global lateral mantle flow and rollback subduction (Carminati and Doglioni, 2012).

Here, we have used the present-day structure of the crust–lithosphere–mantle system to estimate the expected topography

from isostatic compensation, compared this to the observed topography, and thereby estimated the residual topography. This exercise confirms that the variation of crustal thickness cannot explain the variation of topography of the Apennines; we find large magnitude residual topography of ~ 400 m in the Central Apennines and ~ -800 m in the northern Apennines and Calabria. This result is likely to be robust as the along strike comparison implies little sensitivity to the absolute density model. Therefore, we are left to conclude that the residual topography is likely related to the mantle. The mantle contribution to topography may be considered as a “static” process, e.g. due to a difference thickness of the lithosphere mantle, or “dynamic” assuming that it originates from dynamic stresses produced by convection. Both solutions can be fit to the observations. Imposing a thin lithospheric mantle of ~ 70 km beneath the central Apennines and a thick mantle lithosphere of about ~ 140 km beneath the northern Apennines and Calabria would adequately explain the difference in residual topography. This value may be considered as an “effective lithospheric thickness” that is the product of the thickness and density of the mantle lithosphere needed to obtain no residual topography. The comparison between the depth of the effective lithosphere with the receiver function data shows that this solution cannot be excluded.

The alternative, “dynamic” scenario is derived from a circulation calculation based on conversion of the seismic velocity to density under the assumption of negligible chemical anomalies and other effects such as partial melting. The resulting dynamic topography models indicate the presence of a swell over the central Apennines, on the site of the shallow, low seismic velocity anomaly, and a depressed topography over the northern Apennines and Calabria, above the high seismic velocity (subducting slab) (Figs. 2 and 4). The match between the along-strike trends of the dynamic topography model and residual topography support the idea that shallow, upper mantle convection contributes to the present-day topography.

Comparing topography and residual topography to modern rock uplift rates provides additional insights in the underlying dynamic mechanisms. The vertical GPS data confirm that the Apennines remain active with a complex pattern involving both uplift and subsidence at variable rates (Figs. 2, 3, 4). Levelling data, which cover a longer time-interval than GPS, show the same trend and magnitude. Geological data, at even longer timescales, also broadly confirm the general rates and patterns (Fig. 3).

For uplift rate, it may be useful to differentiate between isostatically driven vertical motion due to erosion/sedimentation, crustal thickening/thinning, and a dynamically driven component (Eq. (5)). For example, in the active foreland region of the Po Plain and northern Adriatic, a large part of the subsidence may be explained by flexural bending and sediment loading (Royden et al., 1987). In the mountain belt itself, the isostatic component of the uplift may be related to ongoing crustal thickening, to erosional unloading, or a combination of both. Crustal thickening is ongoing in the northern Apennines and in Calabria and can be estimated from the geodetically determined shortening rate (although this is not straightforward if crustal thickening is occurring in response to deep structural underplating). Current estimates of shortening over the northern Apennines are of the order of ~ 0.5 to 1.5 mm/yr (Serpelloni et al., 2005; Bennett et al., 2012). Such rates will produce uplift on the pro-wedge of the mountain belt of ~ 0.1 mm/yr. Geological estimate on recent deformation of the northern Apennines front gives ~ 2.5 mm/yr shortening resulting on an uplift rate of ~ 1 mm/yr (Picotti and Pazzaglia, 2008). Similarly, extension on the narrower retro-wedge is faster and could produce subsidence of ~ 0.2 mm/yr. In the central-southern Apennines, no contraction is observed and so we expect only the contribution from crustal thinning, producing overall subsidence of 0.1 to 0.3 mm/yr (Patacca

et al., 1990; D’Agostino et al., 2008, 2011a, 2011b). For Calabria, it is more difficult to provide constraints, given the narrow width of the Calabria peninsula, but we expect subsidence due to the ~ 1.5 mm/yr of extension (Serpelloni et al., 2010; D’Agostino et al., 2011a, 2011b), although this might be partially countered by uplift in response to crustal underplating (Piana Agostinetti et al., 2009; Minelli and Faccenna, 2010).

Erosional unloading and isostatic uplift in response can be estimated from a combination of thermochronometry, cosmogenic isotope concentrations, and sediment yield in rivers. Erosion in the northern Apennines has been estimated between 0.2 and 0.4 mm/yr from cosmogenic isotope concentrations, which average the erosion rate over the Holocene (Cyr and Granger, 2008). Thermochronometry, based primarily on apatite fission track dating and (U–Th)/He ages from apatite yields a higher rate of ~ 1 mm/yr in the pro-wedge and ~ 0.3 mm/yr on the retro-wedge in the 3–5 Ma interval (Zattin et al., 2002; Thomson et al., 2010). Therefore, the small positive uplift signal in the northern Apennines may be accounted for by crustal shortening and erosion, while at least part of the negative signal in the foreland region may be explained by subduction and sediment loading (Royden et al., 1987). Interestingly, the erosional component of uplift appears to be larger than the subsidence due to extension, which explains the uplifted marine terraces on the Tyrrhenian coast. In Calabria, thermochronology data show that erosion is limited as the mainland emerged from the sea only recently (since the Lower Pleistocene; Olivetti et al., 2012). Cosmogenic isotope studies indicate that erosion rates are highly variable from ~ 0.01 mm/yr to 1 mm/yr (Cyr et al., 2010; Olivetti et al., 2012). The low rate is found on the plateau and is comparable with apatite fission track thermochronology, which shows denudation rates of ~ 0.1 – 0.2 mm/yr over the last 15–20 Ma (Thomson, 1998). These values are indicative of a young and rapidly uplifting relief. The Aspromonte area (section in Fig. 3c), where subduction is still active, is uplifting at a lower rate than it surrounding place (Faccenna et al., 2011).

In the central-southern Apennines, thermochronometry and cosmogenic isotope studies are rare, due to the dominance of carbonate bedrock. There are some isolated fission track ages in the southern Apennines that indicate erosion rates similar to the northern Apennines (Mazzoli et al., 2008). Sediment yield studies of rivers draining into the Adriatic also show no large change in erosion rate from northern to central Apennines with an average erosion rate of ~ 0.7 mm/yr (Bartolini et al., 1996).

To summarize, the recent Holocene erosion rates across the eastern, pro-wedge flank of the Apennines and Calabria appear to be between ~ 0.5 and 1 mm/yr. Erosion rates on the western, extensional flank appear lower, perhaps by a factor of ~ 2 . Given the uncertainties in these rates, we cannot differentiate rates within each region, but rates appear to be similar from north to south. Including the isostatic factor (Eq. (5)), the contribution to the uplift from erosion is ~ 0.3 to 0.8 mm/yr. Crustal thickening is contributing ~ 0.1 mm/yr uplift to the north Apennine pro-wedge, with an unconstrained component of uplift to the Calabria pro-wedge, and ~ 0.2 mm/yr subsidence to the extensional regions.

Although a significant component of the uplift rate appears to be due to erosion or crustal thickening, the along strike variability that can be resolved supports higher uplift rates in the central Apennines. Both erosion rates and crustal thickening rates are likely higher in the north and lower in the central-southern Apennines. The geodetic uplift rate data show the opposite trend, suggesting the remaining component of the uplift rate, the dynamic uplift rate, arising from changes in mantle flow patterns, is contributing significantly to the central Apennine surface uplift rate. Preliminary dynamic models indeed support the observed trend of uplift (Rozel et al., 2012). However, as the uplift rates are dependent upon poorly constrained parameters such as mantle and

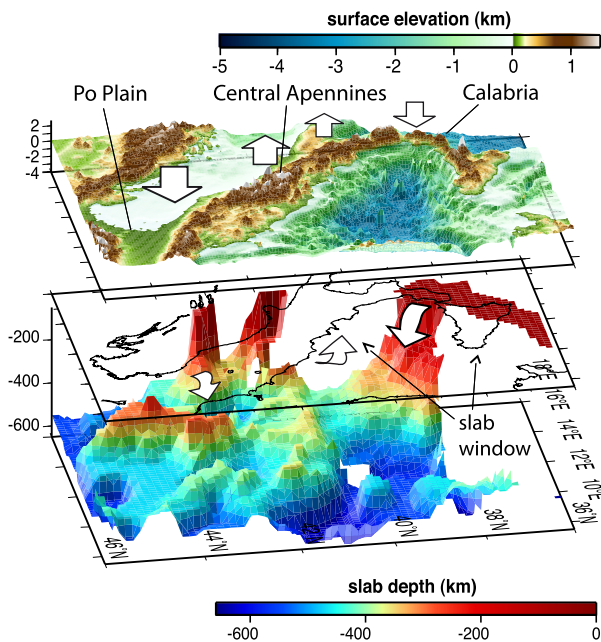


Fig. 5. 3D view of the topography on top of the isosurface enclosing the $>0.8\%$ anomaly volume from P wave M01 tomography model (Piomallo and Morelli, 2003), where the colors indicate depth in km. Notice the correspondence between low topography and locations of active subduction with attached slab segments and the slab window beneath the Central-Southern Apennines. Modified from Faccenna et al. (2011).

lithosphere viscosities, a complete investigation of the parameter space is required to obtain a robust result for the dynamically-induced uplift rate.

6.2. The evolution of the Apennines

Can we relate the topography of the belt to its vertical motion? And are the short-term, vertical geodetic rates representative of recent geological processes? The good match in trend between topography and geodetic uplift rate support this possibility. Using the observed average rate, as in Fig. 4a, we may speculate that at a rate of ~ 0.2 mm/yr, the positive ~ 400 m dynamic topography of the central Apennines may be attained in ~ 2 Myrs. Intriguingly, this time period is in agreement with what has been proposed for the tectonic evolution of the Apennines. Paleomagnetic data show that the bending of the northern Apennines arc mostly occurred during the Pliocene (Speranza et al., 1997) and can be possibly related to that the cessation of subduction in the central Apennines (Lucente and Speranza, 2001). Foredeep flexural deposits in central Apennines fill rapidly subsiding basins during the Neogene and the final cessation of the central Apennines thrust system is completed by the Lower–Middle Pleistocene boundary (Patacca et al., 1990). Therefore, the cessation of subduction, and slab breakoff should have started in the central Apennines in the Early-Pleistocene, at ~ 2.5 – 1.8 Ma (Mattei et al., 2007), propagating southward between 1.5 and 1 Ma (Mattei et al., 2004, 2007). The slab breakoff most probably induced the ultrafast opening of the Marsili basin (Nicolosi et al., 2006), rapid subsidence of the Tyrrhenian region (Kastens et al., 1988), and rapid rollback of the Calabrian slab (Faccenna et al., 2005; Chiarabba et al., 2008).

Summing up, we consider that the mantle component to both topography and uplift rate of the Apennines is best explained by a dynamic process, because: i) the dynamic topography signal resembles the residual topography (Fig. 4a), ii) subduction, although at reduced rate, is still active beneath Calabria and the northern

Apennines, supporting the concept of a convection-related contribution, iii) uplift rate shows a similar trend to the residual/dynamic topography, and, iv) the timescale of the process in the Apennines is too fast to be reconciled with thermal erosion of the lithospheric mantle (Avigad and Gvirtzman, 2009). In this interpretation, the different evolution of the segments of the Apennines is then likely related to the release of the load of the subducting slab on the central Apennines and the subsequent increase in pull of the remaining attached portions of the slab (Guillaume et al., 2010). The history of deformation of the Apennines thus indicates that rapid uplift in its central part occurred after the main phases of crustal thickening, once the pull of the slab disappeared due to its detachment (Figs. 2d, 5, 6). Geological data show that this type of surface evolution has probably been active during the last ~ 1 – 2 Myrs. The fact that surface velocities are similar in pattern to the dynamic topography signal indicates that the process occurring now has evolved as the subduction window in the Central Apennines has grown over time (Fig. 6). This process will probably continue until the subduction window enlarges laterally to a point of complete loss of slab force transmission, i.e. detachment, beneath Calabria and northern Apennines.

This sequence of events illustrates that uplift of mountain belts may have a significant contribution from mantle dynamics during and after crustal thickening. In addition to the Apennines, the western Alps (e.g. Champagnac et al., 2007) and the Atlas mountains (e.g. Teixell et al., 2005; Miller and Becker, 2014) are both under-compensated; their crustal thickness is not large enough given their elevation nor the observed recent uplift. In the western Alps, the latest phase of uplift and exhumation may be due to a process similar to the one that appears active beneath the central Apennines, i.e. a mantle upwelling following a detached slab (Kissling et al., 2006). In the Atlas, slab segmentation appears to have triggered removal of lithosphere (e.g. Duggen et al., 2009), but additional inflow of hot plume material may be required (e.g. Teixell et al., 2005; Miller and Becker, 2014). In contrast, atop active subduction systems such as the Andes (Davila et al., 2010) and the Cascades (Becker et al., 2014) active subduction dynamically depresses the arc–forearc system by ~ 1 km, similarly to what is observed in the northern Apennines–Calabria.

If our interpretation holds, those example orogenic settings may indicate that the commonly adopted assumption of equilibrium due to crustal isostasy cannot explain the elevation of mountain belts alone. Mantle and subduction may reshape the surface at rates as fast as tectonic rates; if so, the cause of the late “epeirogenic” uplift of mountain belts may primarily result from the deformation related to the subducted lithosphere in the upper mantle.

7. Summary and conclusions

We analyzed different contributions for the topography and vertical motion of the Apennines–Calabria belt. We first estimated the isostatic component of topography on the basis of recent receiver function based estimates of crustal thickness. This simple exercise shows that Moho depth is anti-correlated with topography; beneath the Central Apennines crustal thickness is lower and topography higher than for the Northern Apennines and Calabria. This implies that mantle dynamics is contributing to mountain belt topography. This mantle contribution can be an isostatic process, e.g. due to differences in the thickness of the lithospheric mantle, or “dynamic” assuming that it arises from stress produced by present-day convection. The first option requires variations in the thickness of the mantle lithosphere from depths of ~ 150 km beneath Calabria and the northern Apennines to as little as ~ 50 km beneath the Central Apennines. The second option implies dynamic mantle upwelling in the central Apennines and downwelling in the

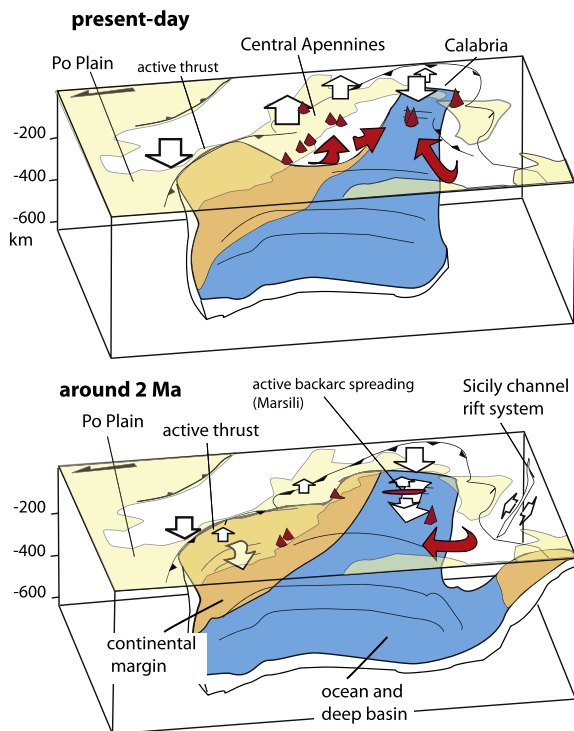


Fig. 6. Two stage interpretative scenarios for the evolution of the subduction system beneath the Central Apennines. Note the rapid development of the slab windows.

northern Apennines and Calabria, likely due to subduction zone reorganization and slab detachment under the central Apennines. We favour this second option because, i) subduction is still active in northern Apennines/Calabria, implying active convection, ii) dynamic topography estimates show patterns similar to the residual topography, and, iii) vertical motions as estimated by both geodetic and geological data indicate that the central Apennines are undergoing higher uplift rates with respect to the surrounding region. These lines of evidence suggest that the Apennines are at least partially dynamically supported by the convecting mantle.

Acknowledgements

We thank Leigh Royden, Zohar Gvirtzman and Yanick Ricard for their constructive reviews. We also thank Claudio Chiarabba for discussion, Claudia Piromallo and Jenny Giacomuzzi for sharing their tomography models, Benjamin Guillaume for Fig. 5, Peter Molnar for constructive comments on the potential role of dynamic topography. C.F. supported from PRIN (2012–2015) project “Uplift and erosion of the Calabrian arc” and TOPOMOD project. T.W.B. was supported by NSF EAR-1215720, M.S.M. was supported by NSF CAREER EAR-1054638. E.S. was partially supported by the PRIN project “Response of morphoclimatic system dynamics to global changes and related geomorphologic hazard”.

Appendix A. Supplementary material

Supplementary material related to this article can be found online at <http://dx.doi.org/10.1016/j.epsl.2014.09.027>.

References

Altamimi, Z., Collilieux, X., Métivier, L., 2011. ITRF2008: an improved solution of the International Terrestrial Reference Frame. *J. Geod.* 85, 457–473. <http://dx.doi.org/10.1007/s00190-011-0444-4>.

Angelica, C., Bonforte, A., Distefano, G., Serpelloni, E., Gresta, S., 2013. Seismic potential in Italy from integration and comparison of seismic and geodetic strain rates. *Tectonophysics* 608, 996–1006.

Avigad, D., Gvirtzman, Z., 2009. Late Neoproterozoic rise and fall of the northern Arabian–Nubian Shield: the role of lithospheric mantle delamination and subsequent thermal subsidence. *Tectonophysics* 477, 217–228.

Bally, A.W., Burbi, L., Cooper, C., Ghelardoni, R., 1986. Balanced sections and seismic reflection profiles across the Central Apennines. *Mem. Soc. Geol. Ital.* 35, 257–310.

Bartolini, C., Caputo, R., Pieri, M., 1996. Pliocene–Quaternary sedimentation in the Northern Apennine Foredeep and related denudation. *Geol. Mag.* 133, 255–273.

Bartolini, C., D’Agostino, N., Dramis, F., 2003. Topography, exhumation, and drainage network evolution of the Apennines. *Episodes* 26 (3), 212–216.

Becker, T.W., Faccenna, C., 2011. A mantle conveyor belt beneath colliding continents. *Earth Planet. Sci. Lett.* 310 (3–4), 453–461.

Becker, T.W., Faccenna, C., Humphreys, E.D., Lowry, A.R., Miller, M.S., 2014. Static and dynamic support of western U.S. topography. *Earth Planet. Sci. Lett.* 402, 234–246.

Bennett, R.A., Serpelloni, E., Hreinsdóttir, S., Brandon, M.T., Buble, G., Basic, T., Casale, G., Cavaliere, A., Anzidei, M., Marjonovic, M., Minelli, G., Molli, G., Montanari, A., 2012. Syn-convergent extension observed using the RETREAT GPS network, northern Apennines, Italy. *J. Geophys. Res.* 117. <http://dx.doi.org/10.1029/2011JB008744>.

Bianchi, I., Park, J., Piana Agostinetti, N., Levin, V., 2010. Mapping seismic anisotropy using harmonic decomposition of receiver functions: an application to Northern Apennines, Italy. *J. Geophys. Res.* 115. <http://dx.doi.org/10.1029/2009JB007061>.

Bigi, S., Lenci, F., Doglioni, C., Moore, J.C., Carminati, E., Scrocca, D., 2003. Decollement depth vs accretionary prism dimension in the Apennines and the Barbados. *Tectonics* 22, 1010. <http://dx.doi.org/10.1029/2002TC001410>.

Carminati, E., Doglioni, C., 2012. Alps vs. Apennines: the paradigm of a tectonically asymmetric Earth. *Earth-Sci. Rev.* 112, 67–96.

Carminati, E., Doglioni, C., Scrocca, D., 2003. Apennines subduction-related subsidence of Venice (Italy). *Geophys. Res. Lett.* 30 (13), 1717. <http://dx.doi.org/10.1029/2003GL017001>.

Casero, P., Roure, F., Vially, R., 1991. Tectonic framework and petroleum potential of the Southern Apennines accretionary wedge. In: Spencer, A.M. (Ed.), *Generation, Accumulation and Production of Europe’s Hydrocarbons*. In: Special Publication of the European Association of Petroleum Geoscientists, vol. 1. Oxford University Press, pp. 381–387.

Cavinato, G.P., De Celles, P.G., 1999. Extensional basins in the tectonically bimodal central Apennine belt, fold-thrust, Italy: response to corner flow above a subducting slab in retrograde motion. *Geology* 27, 955–958.

Cenni, N., et al., 2013. Present vertical movements in central and northern Italy from GPS data: possible role of natural and anthropogenic causes. *J. Geodyn.* 71, 74–85.

Champagnac, J.D., Molnar, P., Anderson, R.S., Sue, C., Delacou, B., 2007. Quaternary erosion-induced isostatic rebound in the western Alps. *Geology* 35, 195–198. <http://dx.doi.org/10.1130/G23053A.1>.

Chiarabba, C., Jovane, L., Di Stefano, R., 2005. A new view of the Italian seismicity using 20 years of instrumental recordings. *Tectonophysics* 395, 251–268.

Chiarabba, C., De Gori, P., Speranza, F., 2008. The southern Tyrrhenian subduction zone: deep geometry, magmatism and Plio-Pleistocene evolution. *Earth Planet. Sci. Lett.* 268 (3–4), 408–423.

Cyr, A.J., Granger, D.E., 2008. Dynamic equilibrium among erosion, river incision, and coastal uplift in the northern and central Apennines, Italy. *Geology* 36 (2), 103–106. <http://dx.doi.org/10.1130/G24003A.1>.

Cyr, A.J., Granger, D.E., Olivetti, V., Molin, P., 2010. Quantifying rock uplift rates using channel steepness and cosmogenic nuclide-determined erosion rates: examples from northern and southern Italy. *Lithosphere* 2, 188–198.

D’Agostino, N., McKenzie, D., 1999. Convective support of long wavelength topography in the Apennines (Italy). *Terra Nova* 11, 234–238.

D’Agostino, N., Jackson, J.A., Dramis, F., Funicello, R., 2001. Interactions between mantle upwelling, drainage evolution and active normal faulting: an example from the central Apennines (Italy). *Geophys. J. Int.* 147 (2), 475–497. <http://dx.doi.org/10.1046/j.1365-246X.2001.00539.x>.

D’Agostino, N., Avallone, A., Cheloni, D., D’Anastasio, E., Mantenuto, S., Selvaggi, G., 2008. Active tectonics of the Adriatic region from GPS and earthquake slip vectors. *J. Geophys. Res.* 113, B12413. <http://dx.doi.org/10.1029/2008JB005860>.

D’Agostino, N., Mantenuto, S., D’Anastasio, E., Giuliani, R., Mattone, M., Calcaterra, S., Gambino, P., Bonci, L., 2011a. Evidence for localized active extension in the central Apennines (Italy) from global positioning system observations. *Geology* 39, 291–294.

D’Agostino, N., D’Anastasio, E., Gervasi, A., Guerra, I., Nedimović, M.R., Seeber, L., Steckler, M., 2011b. Forearc extension and slow rollback of the Calabrian Arc from GPS measurements. *Geophys. Res. Lett.* 38, L17304. <http://dx.doi.org/10.1029/2011GL048270>.

D’Anastasio, E., De Martini, P.M., Selvaggi, G., Pantosti, D., Marchioni, A., Maseroli, R., 2006. Short-term vertical velocity field in the Apennines (Italy) revealed by geodetic levelling data. *Tectonophysics* 418, 219–234.

Dávila, F.M., Lithgow-Bertelloni, C., Giménez, M., 2010. Tectonic and dynamic controls on the topography and subsidence of the Argentine Pampas: the role of the flat slab. *Earth Planet. Sci. Lett.* 295 (1–2), 187–194.

Devoti, R., et al., 2011. Evidence of large scale deformation patterns from GPS data in the Italian subduction boundary. *Earth Planet. Sci. Lett.* 311, 1–12.

- Di Luzio, E., Mele, G., Tiberti, M.M., Cavinato, G.P., Parotto, M., 2009. Moho deepening and shallow upper crustal delamination beneath the central Apennines. *Earth Planet. Sci. Lett.* 280, 1–12.
- Di Stefano, R., et al., 2011. Three-dimensional Moho topography in Italy: new constraints from receiver functions and controlled source seismology. *Geochem. Geophys. Geosyst.* 12 (9), Q09006.
- Dogliani, C., Merlini, S., Cantarella, G., 1999. Foredeep geometries at the front of the Apennines in the Ionian sea (central Mediterranean). *Earth Planet. Sci. Lett.* 168 (3–4), 243–254.
- Duggen, S., Hoernle, K.A., Hauff, F., Klügel, A., Bouabdellah, M., Thirlwall, M., 2009. Flow of Canary mantle plume material through a subcontinental lithospheric corridor beneath Africa to the Mediterranean. *Geology* 37, 283–286.
- Faccenna, C., Becker, T.W., 2010. Shaping mobile belt from small scale convection. *Nature* 465. <http://dx.doi.org/10.1038/nature09064>.
- Faccenna, C., Civetta, L., D'Antonio, M., Funicello, F., Margheriti, L., Piromallo, C., 2005. Constraints on mantle circulation around the deforming Calabrian slab. *Geophys. Res. Lett.* 32, L06311. <http://dx.doi.org/10.1029/2004GL021874>.
- Faccenna, C., Molin, P., Orecchio, B., Olivetti, V., Bellier, O., Funicello, F., Minelli, L., Piromallo, C., Billi, A., 2011. Topography of the Calabria subduction zone (southern Italy): Clues for the origin of Mt. Etna. *Tectonics* 30, TC1003. <http://dx.doi.org/10.1029/2010TC002694>.
- Faure Walker, J.P., Roberts, G.P., Cowie, P.A., Papanikolaou, I., Michetti, A.M., Sammonds, P., Wilkinson, M., McCaffrey, K.J.W., Phillips, R.J., 2012. Relationship between topography, rates of extension and mantle dynamics in the actively-extending Italian Apennines. *Earth Planet. Sci. Lett.* 325–326, (ISSN 0012-821X), 76–84. <http://dx.doi.org/10.1016/j.epsl.2012.01.028>.
- Ferranti, L., et al., 2006. Markers of the last interglacial sea level highstand along the coast of Italy: tectonic implications. *Quat. Int.* 145–146, 30–54.
- Giacomuzzi, G., Civalieri, M., De Gori, P., Chiarabba, C.A., 2012. 3D vs model of the upper mantle beneath Italy: insight on the geodynamics of central Mediterranean. *Earth Planet. Sci. Lett.* 335–336, 105–120.
- Guillaume, B., Funicello, F., Faccenna, C., Martinod, J., Olivetti, V., 2010. Spreading pulses of the Tyrrhenian Sea during the narrowing of the Calabrian slab. *Geology* 38 (9), 819–822. <http://dx.doi.org/10.1130/G31038.1>.
- Gurnis, M., Mitrovica, J.X., Ritsema, J., vanHeijst, H.J., 2000. Constraining mantle density structure using geological evidence of surface uplift rates: the case of the African superplume. *Geochem. Geophys. Geosyst.* 1, 1020. <http://dx.doi.org/10.1029/1999GC000035>.
- Gutscher, M., Roger, J., Baptista, M., Miranda, J., Tinti, S., 2006. Source of the 1693 Catania earthquake and tsunami (southern Italy): new evidence from tsunami modeling of a locked subduction fault plane. *Geophys. Res. Lett.* 33.
- Gvirtzman, Z., Nur, A., 2001. Residual topography, lithospheric structure and sunken slabs in the central Mediterranean. *Earth Planet. Sci. Lett.* 187, 117–130.
- Hager, B.H., 1984. Subducted slabs and the geoid: constraints on mantle rheology and flow. *J. Geophys. Res.* 89, 6003–6015.
- Hager, B.H., Clayton, R.W., Richards, M.A., Comer, R.P., Dziewonski, A.M., 1985. Lower mantle heterogeneity, dynamic topography and the geoid. *Nature* 313, 541–545. <http://dx.doi.org/10.1038/313541a0>.
- Houseman, G., McKenzie, D., Molnar, P., 1981. Convective instability of a thickened boundary layer and its relevance for the thermal evolution of continental convergent belts. *J. Geophys. Res.* 86, 6115–6132.
- Karner, G.D., Watts, A.B., 1983. Gravity anomalies and flexure of the lithosphere at mountain ranges. *J. Geophys. Res., Solid Earth* 88 (B12), 10449–10477.
- Kastens, K.A., Mascle, J., O.D.P. Scientific Party, 1988. ODP Leg 107 in the Tyrrhenian Sea: insights into passive margin and back arc basin evolution. *Geol. Soc. Am. Bull.* 100, 1140–1156.
- Kissling, E., Schmid, S., Lippitsch, R., Ansorge, J., Fugenschuh, B., 2006. Lithosphere structure and tectonic evolution of the Alpine arc: new evidence from high-resolution teleseismic tomography. *Mem. Geol. Soc. Lond.* 32, 129–145.
- Lachenbruch, A.H., Morgan, P., 1990. Continental extension, magmatism and elevation; formal relations and rules of thumb. *Tectonophysics* 174, 39–62.
- Lambeck, K., Smither, C., Johnston, P., 1988. Sea-level change, glacial rebound and mantle viscosity for northern Europe. *Geophys. J. Int.* 134, 102–144.
- Le Stunff, Y., Ricard, Y., 1995. Topography and geoid due to mass anomalies. *Geophys. J. Int.* 122, 982–990.
- Li, C., van der Hilst, R.D., Engdahl, E.R., Burdick, S., 2008. A new global model for P wave speed variations in Earth's mantle. *Geochem. Geophys. Geosyst.* 9, Q05018. <http://dx.doi.org/10.1029/2007GC001806>.
- Lucente, F.P., Speranza, F., 2001. Belt bending driven by lateral bending of subducting lithospheric slab: geophysical evidences from the northern Apennines (Italy). *Tectonophysics* 337 (1–2), 53–64.
- Lucente, F.P., Chiarabba, C., Cimini, G.B., Giardini, D., 1999. Tomographic constraints on the geodynamic evolution of the Italian region. *J. Geophys. Res.* 104, 20307–20327.
- Malinverno, A., Ryan, W.B.F., 1986. Extension on the Tyrrhenian Sea and shortening in the Apennines as results of arc migration driven by sinking of the lithosphere. *Tectonics* 5, 227–245.
- Mattei, M., Petrocelli, V., Lacava, D., Schiattarella, M., 2004. Geodynamic implications of Pleistocene ultrarapid vertical-axis rotations in the Southern Apennines, Italy. *Geology* 32 (9), 789–792.
- Mattei, M., Cifelli, F., D'Agostino, N., 2007. The evolution of the Calabrian arc: evidence from paleomagnetic and GPS observations. *Earth Planet. Sci. Lett.* 263, 259–274. <http://dx.doi.org/10.1016/j.epsl.2007.08.034>.
- Mazzoli, S., Dapos, E., Aldega, L., Corrado, S., Invernizzi, C., Shiner, P., Zattin, M., 2008. Tectonic burial and “young” (<10 Ma) exhumation in the southern Apennines fold-and-thrust belt (Italy). *Geology* 36, 243.
- Mele, G., Sandvol, E., Cavinato, G., 2006. Evidence of crustal thickening beneath the central Apennines (Italy) from teleseismic receiver functions. *Earth Planet. Sci. Lett.* 249, 425–435.
- Miller, M.S., Becker, T.W., 2014. Reactivated lithospheric-scale discontinuities localize dynamic uplift of the Moroccan Atlas Mountains. *Geology* 42, 35–38.
- Miller, M.S., Piana Agostinetti, N., 2012. Insights into the evolution of the Italian lithospheric structure from S receiver function analysis. *Earth Planet. Sci. Lett.* 348, 49–59.
- Minelli, L., Faccenna, C., 2010. Evolution of the Calabrian accretionary wedge, central Mediterranean. *Tectonics* 29, TC4004. <http://dx.doi.org/10.1029/2009TC002562>.
- Mitrovica, J.X., Beaumont, C., Jarvis, G.T., 1989. Tilting of continental interiors by the dynamical effects of subduction. *Tectonics* 8, 1079–1094.
- Molnar, P., England, P., 1990. Late Cenozoic uplift of mountain range and global climate: chicken or egg? *Nature* 346, 29–34.
- Montone, P., Mariucci, M.T., Pondrelli, S., Amato, A., 2004. An improved stress map for Italy and surrounding regions (Central Mediterranean). *J. Geophys. Res.* 109, B10410.
- Mostardini, F., Merlini, S., 1986. Appennino centro-meridionale. Sezioni geologiche e proposta di modello strutturale. *Mem. Soc. Geol. Ital.* 35, 177–202.
- Nicolosi, I., Speranza, F., Chiappini, M., 2006. Ultrafast oceanic spreading of the Marsili basin, southern Tyrrhenian Sea: Evidence from magnetic anomaly analysis. *Geology* 34 (9), 717–720.
- Olivetti, V., Cyr, A.J., Molin, P., Faccenna, C., Granger, D.E., 2012. Uplift history of the Sila Massif, southern Italy, deciphered from cosmogenic ¹⁰Be erosion rates and river longitudinal profile analysis. *Tectonics* 31 (TC3007), 26. <http://dx.doi.org/10.1029/2011TC003037>.
- Panasjuk, S.V., Hager, B.H., 2000. Models of isostatic and dynamic topography, geoid anomalies, and their uncertainties. *J. Geophys. Res.* 105, 28199–28209.
- Patacca, E., Sartori, R., Scandone, P., 1990. Tyrrhenian basin and Apenninic arcs: kinematic relations since late tortonian times. *Mem. Soc. Geol. Ital.* 45, 425–451.
- Pauselli, C., Barchi, M.R., Federico, C., Magnani, B., Minelli, G., 2006. The crustal structure of the Northern Apennines (Central Italy): an insight by the Crop03 seismic line. *Am. J. Sci.* 306, 428–450. <http://dx.doi.org/10.2475/06.2006.02>.
- Peltier, W.R., 2004. Global glacial isostasy and the surface of the Ice-Age Earth: the ICE-5G (VM2) model and GRACE. *Annu. Rev. Earth Planet. Sci.* 32 (1), 111–149.
- Piana Agostinetti, N., Amato, A., 2009. Moho depth and Vp/Vs ratio in peninsular Italy from teleseismic receiver functions. *J. Geophys. Res.* 114, B06303.
- Piana Agostinetti, N., Steckler, M.S., Lucente, F.P., 2009. Imaging the subducted slab under the Calabrian Arc, Italy, from receiver function analysis. *Lithosphere* 1, 131–138. <http://dx.doi.org/10.1130/L49.1>.
- Piana Agostinetti, N., Bianchi, I., Amato, A., Chiarabba, C., 2011. Fluid migration in continental subduction: the Northern Apennines case study. *Earth Planet. Sci. Lett.* 302, 267–278.
- Picotti, V., Pazzaglia, F.J., 2008. A new active tectonic model for the construction of the northern Apennines mountain front near Bologna (Italy). *J. Geophys. Res.* 113. <http://dx.doi.org/10.1029/2007JB005307>.
- Piromallo, C., Morelli, A., 2003. P-wave tomography of the mantle under the Alpine-Mediterranean area. *J. Geophys. Res.* 108 (B2), 2065.
- Pizzi, A., 2003. Plio-Quaternary uplift rates in the outer zone of the central Apennines fold-and-thrust belt, Italy. *Quat. Int.* 101–102, 229–237.
- Ricard, Y., Fleitout, L., Froidevaux, C., 1984. Geoid heights and lithospheric stresses for a dynamic Earth. *Ann. Geophys.* 2, 267–286.
- Ricard, Y., Richards, M.A., Lithgow-Bertelloni, C., Lestunff, Y., 1993. A geodynamic model of mantle mass heterogeneities. *J. Geophys. Res.* 98, 21895–21909.
- Royden, L.H., 1993. The tectonic expression slab pull at continental convergent boundaries. *Tectonics* 2, 303–325. <http://dx.doi.org/10.1029/92TC02248>.
- Royden, L., Patacca, E., Scandone, P., 1987. Segmentation and configuration of subducted lithosphere in Italy: an important control on thrust-belt and foredeep-basins evolution. *Geology* 15, 714–717.
- Rozel, A., Becker, T.W., Faccenna, C., Funicello, F., Husson, L., 2012. Scaling laws of dynamic topography and uplift rate. In: EGU 2012.
- Scrocca, D., Dogliani, C., Innocenti, F., 2003. Constraints for an interpretation of the Italian geodynamics: a review. In: Scrocca, D., et al. (Eds.), CROP Atlas: Seismic Reflection Profiles of the Italian Crust. In: *Mem. Descr. Carta Geol. It.*, vol. 62, pp. 15–46.
- Serpelloni, E., Anzidei, M., Baldi, P., Casula, G., Galvani, A., 2005. Crustal velocity and strain-rate fields in Italy and surrounding regions: new results from the analysis of permanent and non-permanent GPS networks. *Geophys. J. Int.* 161 (3), 861–880. <http://dx.doi.org/10.1111/j.1365-246X.2005.02618.x>.
- Serpelloni, E., Bürgmann, R., Anzidei, M., Baldi, P., Mastrolombo Ventura, B., Boschi, E., 2010. Strain accumulation across the Messina Straits and kinematics of Sicily and Calabria from GPS data and dislocation modeling. *Earth Planet. Sci. Lett.* 298, 347–360.

- Serpelloni, E., Faccenna, C., Spada, G., Dong, D., Williams, S.P., 2013. Vertical GPS ground motion rates in the Euro-Mediterranean region: new evidence of velocity gradients at different spatial scales along the Nubia–Eurasia plate boundary. *J. Geophys. Res.* 118 (11), 6003–6024.
- Shaw, M., Pysklywec, R., 2007. Anomalous uplift of the Apennines and subsidence of the Adriatic: the result of active mantle flow? *Geophys. Res. Lett.* 34, L04311.
- Simmons, N.A., Forte, A.M., Boschi, L., Grand, S.P., 2010. GYPsuM: a joint tomographic model of mantle density and seismic wave speeds. *J. Geophys. Res.* 115, B12310.
- Speranza, F., Sagnotti, L., Mattei, M., 1997. Tectonics of the Umbria–Marche–Romagna Arc (central northern Apennines, Italy): new paleomagnetic constraints. *J. Geophys. Res.* 102 (B2), 3153–3166.
- Steinberger, B., Calderwood, A., 2006. Models of large-scale viscous flow in the earth's mantle with constraints from mineral physics and surface observations. *Geophys. J. Int.* 167, 1461–1481.
- Teixell, A., et al., 2005. Effects of mantle upwelling in a compressional setting: the Atlas Mountains of Morocco. *Terra Nova* 17, 456–461.
- Thomson, S.N., 1998. Assessing the nature of tectonic contact using fission track thermochronology: an example from the Calabrian Arc, southern Italy. *Terra Nova* 10, 32–36. <http://dx.doi.org/10.1046/j.1365-3121.1998.00165.x>.
- Thomson, S.N., Brandon, M.T., Reiners, P.W., Zattin, M., Isaacson, P.J., Balestrieri, M.L., 2010. Thermochronologic evidence for orogen-parallel variability in wedge kinematics during extending convergent orogenesis of the northern Apennines, Italy. *Geol. Soc. Am. Bull.* 1 (21).
- Westaway, R., 1993. Quaternary uplift of southern Italy. *J. Geophys. Res.* 98, 21741–21772.
- Wortel, M.J.R., Spakman, W., 2000. Subduction and slab detachment in the Mediterranean–Carpathian region. *Science* 290, 1910–1917.
- Zattin, M., Picotti, V., Zuffa, G., 2002. Fission-track reconstruction of the front of the Northern Apennine thrust wedge and overlying Ligurian unit. *Am. J. Sci.* 302, 346–379.